THE JOURNAL OF BIOLOGICAL CHEMISTRY VOL. 286, NO. 12, pp. 10329–10340, March 25, 2011

A Novel Member of the RNase D Exoribonuclease Family Functions in Mitochondrial Guide RNA Metabolism in *Trypanosoma brucei*[*] [S]

Received for publication, June 7, 2010, and in revised form, January 18, 2011 Published, JBC Papers in Press, January 20, 2011, DOI 10.1074/jbc.M110.152439

Sara L. Zimmer[‡], Sarah M. McEvoy[‡], Jun Li[§], Jun Qu[§], and Laurie K. Read[‡1]

From the [‡]Department of Microbiology and Immunology, School of Medicine and Biomedical Sciences, University at Buffalo, Buffalo, New York 14214 and the [§]Department of Pharmaceutical Sciences, University at Buffalo, State University of New York, Amherst, New York 14260

RNA turnover and RNA editing are essential for regulation of mitochondrial gene expression in *Trypanosoma brucei*. RNA turnover is controlled in part by RNA 3′ adenylation and uridylation status, with *trans*-acting factors also impacting RNA homeostasis. However, little is known about the mitochondrial degradation machinery or its regulation in *T. brucei*. We have identified a mitochondrial exoribonuclease, TbRND, whose expression is highly up-regulated in the insect proliferative stage of the parasite. TbRND shares sequence similarity with RNase D family enzymes but differs from all reported members of this family in possessing a CCHC zinc finger domain. *In vitro*, TbRND exhibits 3′ to 5′ exoribonuclease activity, with specificity toward uridine homopolymers, including the 3′ oligo(U) tails of guide RNAs (gRNAs) that provide the sequence information for RNA editing. Several lines of evidence generated from RNAi-mediated knockdown and overexpression cell lines indicate that TbRND functions in gRNA metabolism *in vivo*. First, TbRND depletion results in gRNA tails extended by 2–3 nucleotides on average. Second, overexpression of wild type but not catalytically inactive TbRND results in a substantial decrease in the total gRNA population and a consequent inhibition of RNA editing. The observed effects on the gRNA population are specific as rRNAs, which are also 3′-uridylated, are unaffected by TbRND depletion or overexpression. Finally, we show that gRNA binding proteins co-purify with TbRND. In summary, TbRND is a novel 3′ to 5′ exoribonuclease that appears to have evolved a function highly specific to the mitochondrion of trypanosomes.

Recognition of the importance of post-transcriptional processes has changed the way we look at gene regulation (1). RNA degradation that occurs in both substrate processing and turnover is an important aspect of post-transcriptional regulation in all organisms (1–7), and the factors controlling these processes are beginning to be elucidated. Increasingly, we find that 3′ non-encoded tails serve as *cis*-acting elements in RNA stability regulation. Perhaps the most commonly reported examples of this are oligo(A) tails acting in both RNA stabilization and destabilization (5, 8–14). However, oligo(U) tails have also been found to destabilize microRNAs, siRNAs, and decay intermediates and possibly act as quality control mechanisms (15–20). Non-encoded 3′ tails can recruit and influence the activity of exoribonucleases, which along with endoribonucleases, supply the catalytic activity necessary for RNA degradation. Exoribonucleases are organized into a number of different families or classes (21). Some of these enzymes, such as RNase II, PNPase, and Xrn1, exhibit processive activity and participate in overall RNA turnover pathways, although each is a member of a different family. Others, like RNase D, a member of the DEDD class of exoribonucleases, have distributive activity and function in very specific regulatory roles (21–23). In organelles, regulation of RNA stability and the classes of exoribonucleases responsible for both general and regulatory RNA degradation vary greatly between organisms (9, 24). Furthermore, efforts to identify exoribonucleases responsible for mitochondrial RNA degradation have met with limited success (9, 24). A prime example of a mitochondrion that apparently utilizes multiple exoribonucleases, currently unidentified, is that of the kinetoplastids. Kinetoplastid protozoa, including *Trypanosoma brucei*, *T. cruzi*, and *Leishmania* spp., are the causative agents of several deadly human diseases (25). These organisms are named for their unique mitochondrial DNA, called the kinetoplast, which is composed of tens of thousands of catenated circular molecules of two types, maxicircles and minicircles (26). The 20–35-kb maxicircles are analogous to mitochondrial DNA of other organisms, encoding 18 mRNAs and two ribosomal RNAs. The ~1-kb minicircles encode small guide RNAs (gRNAs)[2] that function as *trans*-acting factors in the editing of 12 of 18 maxicircle-encoded mRNAs. gRNAs interact with cognate mRNAs in a sequential and ordered manner, providing the sequence information for the specific uridine insertion and deletion required to create translatable mRNAs. Studies in *T. brucei* indicate that transcription of both maxicircles and minicircles is polycistronic, leaving little room for gene regulation at the level of RNA synthesis (27–30). Nevertheless, the abundance of mature monocistronic mRNAs often varies dramatically between human bloodstream form (BF) and insect procyclic

* This work was supported, in whole or in part, by National Institutes of Health Grant RO1 AI077520 (to L. K. R.).

[S] The on-line version of this article (available at http://www.jbc.org) contains supplemental Table S1 and Fig. S1.

[1] To whom correspondence should be addressed. Fax: 716-829-2158; E-mail: lread@buffalo.edu.

[2] The abbreviations used are: gRNA, guide RNA; BF, bloodstream form; PF, procyclic form; TAP, tandem affinity purification; tet, tetracycline; MHT, Myc/His/TAP; MRB1, mitochondrial RNA binding complex 1; nt, nucleotide(s); qRT, quantitative real-time.

form (PF) life cycle stages (27, 30–33), suggesting that the stability of specific RNAs is regulated developmentally and/or in response to external or internal signals. There is also evidence of regulation of the ratio between edited and pre-edited forms of a given mRNA (11, 33–38) that could depend on both the inherent stability of the two forms of the transcript and on regulation of the RNA editing process.

Cis-acting elements that may impact mitochondrial RNA decay in trypanosomes include a variety of non-encoded 3′ tails that are present on almost all RNA classes. Monocistronic maxicircle mRNAs possess 1–40-nt non-encoded oligomer tails, the compositions of which can vary depending on the RNA (11, 33, 39–41). These mRNA 3′ tails appear to regulate RNA stability and decay with differing effects depending on the editing status of the RNA (11, 38, 39, 42). Additionally, long tails of 100 or more nucleotides composed of A/U polymers (11, 39) are added to a limited number of never-edited and edited RNAs and may play a role in translation (11, 43). gRNAs possess non-encoded oligo(U) tails of 5–14 nucleotides (44) that play a role in gRNA function by stabilizing gRNA/mRNA interactions (45–47). Finally, maxicircle-encoded 9 S and 12 S rRNAs also possess oligo(U) tails (39, 48), although their function is not clear. Thus, non-encoded 3′ tails of kinetoplastid mitochondrial RNAs likely compose part of a complex network of RNA stabilization and destabilization pathways and play a critical role in gene regulation. Presumably, these 3′ non-encoded tails serve as targets for *trans*-acting factors, including RNA-binding proteins and ribonucleases that determine the fate of a particular RNA whether that fate would be functionality or decay.

Only three exoribonucleases have been previously described in trypanosome mitochondria. Two of these, KREX1 and KREX2, are apparently devoted to U-deletion RNA editing (49–51). Both are U-specific exoribonucleases and components of the editosome that catalyzes RNA editing (52–56). The only non-editosome mitochondrial exoribonuclease that has been studied in detail is the RNR family enzyme, TbDSS-1 (57–59). TbDSS-1 interacts with the RNA helicase, TbSUV3, and functions in RNA surveillance and decay of non-functional byproducts of primary transcript processing. In addition, down-regulation TbDSS-1 leads to a range of pleiotropic effects on mitochondrial RNA populations that are not well understood.

The study of mitochondrial exoribonucleases is integral to our understanding of mitochondrial gene regulation and will provide insight into the roles of non-encoded 3′ tails in regulatory pathways. Here, we present *in vitro* and *in vivo* analysis of a novel mitochondrial exoribonuclease that we term TbRND, which is the first organellar member of the RNase D subfamily of the DEDD nucleases (21). *In vitro*, TbRND exhibits U-specific 3′ to 5′ exoribonuclease activity. *In vivo*, the enzyme is mitochondrially-localized and strongly developmentally regulated. Studies in PF *T. brucei* involving both RNAi-mediated knockdown and overexpression demonstrate that gRNAs are a specific target of this enzyme. Overexpression of TbRND results in a depletion of the gRNA population and a consequent inhibition of RNA editing. We also show that tandem affinity purification (TAP)-tagged TbRND associates with several members of the mitochondrial RNA binding complex 1 (MRB1) complex including the GAP1/2 (also known as GRBC1/2) proteins (39, 60, 61), consistent with a role in gRNA metabolism.

EXPERIMENTAL PROCEDURES

cDNA Cloning and Plasmid Construction—Oligonucleotides used for cloning are shown in supplemental Table S1. The gene encoding the TbRND open reading frame (Tb09.211.3670, NCBI accession number EAN77178) was inserted between the HindIII and BamHI sites in the pLEW-MHTAP plasmid (62) to generate pRND-MHT for tetracycline (tet)-regulated expression of TbRND with a C-terminal myc-His_6-TAP tag in *T. brucei*. For expression of tet-inducible RNAi, nucleotides 1–825 of the TbRND gene were cloned into the p2T7–177 plasmid (63) between BamHI and HindIII restriction sites internal to opposing T7 promoters to generate p2T7–177TbRND. For bacterial expression studies, the TbRND open reading frame was cloned into pET42a (Novagen) between 5′ BamHI and 3′ HindIII sites to generate pET-RND, which expresses TbRND with an N-terminal glutathione *S*-transferase (GST)/His tag in *Escherichia coli*. The mutant pET-RND-D80A and pRND-D80A-MHT plasmids were constructed from the TbRND wild type plasmids using the QuikChange II site-directed mutagenesis kit (Stratagene).

T. brucei Cell Culture, Transfection, and Induction and Mitochondrial Extract Preparation—PF *T. brucei* strain 29-13 (from Dr. George A. M. Cross, Rockefeller University), which contains integrated genes for the T7 RNA polymerase and the tet repressor, were grown in SDM-79 media supplemented with 10% fetal bovine serum (FBS) as indicated previously (64). BF single marker *T. brucei* cells (also provided by Dr. George A. M. Cross) were cultured in HMI-9 media supplemented with 10% FBS and 10% Serum Plus (SAFC) (64). To generate a tet-inducible clonal TbRND RNAi cell line, NotI-linearized p2T7–177TbRND was transfected into 29-13 cells, resulting in two phleomycin-resistant polyclonal cultures. Six clones per culture were obtained by limiting dilution and induced with tet at 1×10^6 cells/ml, with cells harvested at day 3 for RNA and protein collection. pRND-MHT was transfected into 29-13 cells, resistant cells were selected by phleomycin, and clones were obtained by limiting dilution. Tet-induced cells at 2×10^6 cells/ml starting concentration were harvested at 2 days for protein and RNA collection. In all cases cells were induced at 2.5 μg/ml tet, and for growth curves, cells were induced at a concentration of 1×10^6 cells/ml and diluted as necessary every 24–48 h. Values from three independent growth experiments were averaged to generate growth curves with experimental error bars depicting S.D. Mitochondrial extract of 29-13 cells was prepared as described (65).

Antibodies and Immunoblotting—Rabbit polyclonal serum was raised against purified recombinant GST-His-TbRND (see below) by Proteintech Group, Inc. (Chicago, IL). TbRND antisera were affinity-purified with GST-his-TbRND bound to nitrocellulose. The purified antisera recognized a band of just >40 kDa in lysates from 29-13 *T. brucei* (supplemental Fig. S1). The entire open reading frame of GAP1 was cloned into pET21A for the expression of His-GAP1 in *E. coli*. Protein purified on a nickel column under denaturing conditions was used

to raise rabbit polyclonal antisera, which were affinity-purified as described above. Affinity-purified GAP1 antisera recognized a band of just >55 kDa in *T. brucei* cell lysates. Affinity-purified polyclonal anti-peptide antibodies against CGASKESDS (Tb927.2.6070, NCBI accession number AAQ16064) were purchased from Bethyl Laboratories. A commercial antibody was used for detection of the Myc tag (Immunology Consultants Laboratory, Inc., Newberg, OR). Anti-HSP70 antibodies were generously provided by James Bangs (University of Wisconsin). Previously described were antibodies against GAP2 (60), MRP2 (66), TbRGG2 (67), PRMT1, PRMT6, and PRMT7 (68). For Western analysis, cells were counted using a hemacytometer, and total cells were pelleted, resuspended in PBS with SDS-PAGE sample buffer, and boiled before SDS-PAGE and immunoblotting. Alternatively, in the case of the cell fractionation experiment, total cell lysates were prepared by passing cells in protein extraction buffer (150 mM sucrose, 20 mM KCl, 3 mM $MgCl_2$, 20 mM HEPES (pH 7.9), 1 mM DTT, and 0.2% Nonidet P-40) 3 times through a 26-gauge needle, and mitochondrial lysates were obtained as described (65). QuantityOne software (Bio-Rad) was used in densitometric analyses of TbRND levels in immunoblots.

Fluorescence Microscopy—Mitochondria were labeled by treating cells with 250 nM MitoTracker Red CMXRos in SDM-79 for 15 min before cell harvest using a modification of the protocol in Engstler and Boshart (69). Briefly, cells were fixed in suspension on ice for 30 min with 4% paraformaldehyde. Fixed cells were incubated for 1 h with Anti-c-Myc (9E10) mouse monoclonal IgG (Santa Cruz Biotechnology) at a dilution of 1:50. Anti-mouse Cy5 conjugated antibody (Chemicon) at a 1:200 dilution was used as a secondary antibody in a 30-min co-incubation with DAPI, and cells were mounted as described. A Zeiss Axioimager Z1 fluorescence microscope and AxioVision software were used to visualize trypanosomes. Cells untreated with Mitotracker and cells untreated with c-Myc were also visualized for each experiment (not shown) to verify that the Mitotracker and Cy5 signals did not overlap.

RNA Extraction, Nucleic Acid Blotting, and Guanylyltransferase Labeling—Total RNA from cells was extracted from uninduced and induced TbRND RNAi and TbRND-MHT cells using TRIzol reagent (Invitrogen). A further phenol/chloroform/isoamyl alcohol (25:24:1) extraction was performed on RNA with A_{260}/A_{280} ratios less than 2.0. For rRNA blots, 2 μg of total RNA was incubated with 2 pmol of the near-3′ end antisense oligo for either 9 S or 12 S (supplemental Table S1), and cleavage with RNase H was performed as described (31). After phenol/chloroform/isoamyl alcohol extraction and ethanol precipitation, one-half of the reaction was loaded on a 30-cm 10% polyacrylamide denaturing gel to separate rRNA 3′ ends to single nucleotide resolution. RNA was then transferred to a charged nylon membrane by semidry transfer in 0.5× Tris borate-EDTA buffer, and the blots were probed with end-labeled DNA oligonucleotides antisense to the extreme encoded 3′ ends of 12 S and 9 S (supplemental Table S1) as described previously (31). Guanylyltransferase labeling was performed as described (70, 71). QuantityOne software (Bio-Rad) was used in densitometric analyses of radiograms generated by scanning rRNA blots and guanylyltransferase-labeled RNA gels with Bio-Rad Personal Imager FX.

qRT-PCR—For qRT-PCR, 4 μg of RNA was treated with a DNase kit (Ambion) to remove any residual DNA. RNA was reverse-transcribed and amplified using a MyiQ single-color real-time PCR detection system as described (72) using primers specific to never edited, pre-edited, edited, and pre-processed RNAs described in Refs. 11 and 72–74.

Bacterially Expressed TbRND Purification and in Vitro RNA Degradation Assay—Bacterial cells harboring the pET42a-RND or pET-RND-D80A plasmids were grown in LB with 2% ethanol to enhance exogenous protein solubility. After growth at 37 °C to an optical density of 0.6, cells were induced with 0.3 mM isopropyl 1-thio-β-D-galactopyranoside and allowed to grow for 20 h at 17 °C. After harvesting, cells were sonicated, and the TbRND fusion protein was purified from crude extracts by sequential affinity chromatography on TALON resin (Clontech) and glutathione-agarose, resulting in nearly pure protein preparations that were quantitated by comparison with BSA standards on Coomassie-stained SDS-PAGE. These proteins and TbRND-MHC (see below) were analyzed in an RNA degradation assay as described (38, 42) with slight modifications. Briefly, a 50-μl reaction volume contained nuclease buffer, 5 mM $MgCl_2$, 0.01 pmol of end-labeled RNA oligonucleotides (51) or end-labeled *in vitro* transcribed gA6[14] (75), and the indicated amounts of the purified enzymes. Reaction mixtures were incubated at 24 °C for the times indicated and stopped by the addition of 5 μl of stop buffer (50 mM EDTA and 0.2% SDS). RNAs were extracted with acidic phenol/chloroform/isoamyl alcohol (25:24:1), and 20 μl of the aqueous layer was added to 20 μl of 90% formamide loading buffer. Samples were heated for 5 min at 95 °C. Equal volumes of each reaction mixture were then analyzed by electrophoresis on 12.5% acrylamide denaturing gels followed by phosphorimaging analysis.

TAP Purification, LC-MS/MS, and Glycerol Gradients—TAP purification of TbRND, PRMT7, and PRMT6 (68) was performed as described in Schimanski *et al.* (76). Purified TbRND-MHC was quantitated by comparison with BSA protein standards on silver-stained SDS-PAGE. 5.6 μg was sent to Seattle BioMed for LC-MS/MS, and 1.5 μg was extensively washed in a YM-10 Microcon concentrator to exchange the calmodulin elution buffer for 50 mM Tris (pH 8) and was concentrated under vacuum to yield a final protein concentration >1.5 mg/ml. The preparation was then subjected to a highly efficient and high-recovery precipitation and an on-pellet digestion procedure described previously (77). Briefly, a dual enzyme and dual activation strategy was employed for a comprehensive proteomic identification. For proteolytic digestion, each purified sample was split, and two enzymes were employed individually in parallel: trypsin (cuts at Lys and Arg) and *Staphylococcus aureus* V8 protease (Glu-c; cuts at Asp and Glu). A high resolution and highly reproducible nano-LC gradients coupled to a LTQ/Orbitrap/ETD analyzer was employed for identification of captured proteins. Data base searching was carried out using the SEQUEST algorithm implemented on a 64-node supercomputer at the University at Buffalo Center for Computation Research. A set of highly stringent criteria were used to minimize false-positive identifications, which includes precur-

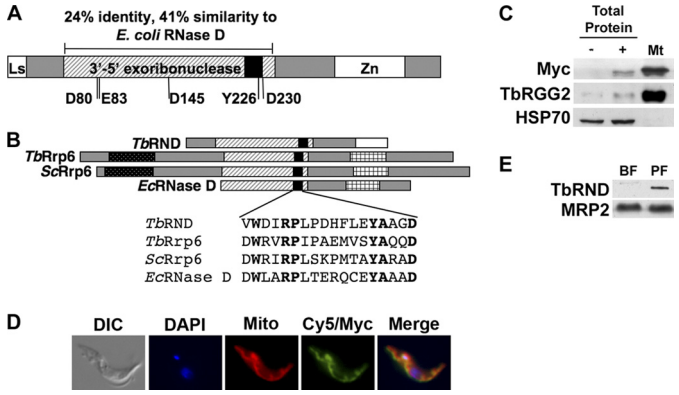

FIGURE 1. **Organization, localization, and expression of TbRND.** *A*, a schematic of TbRND domain structure is shown. *Ls*, predicted mitochondrial localization signal; *Zn*, CCHC zinc finger; *hatched*, 3′ to 5′ exoribonuclease domain; *black*, RNase D motif. TbRND contains all of the conserved residues of the DEDDy family catalytic domain (displayed with *vertical lines below their locations*). The *horizontal line* indicates the region with similarity to *E. coli* RNase D. *B*, alignment of TbRND with selected members of the RND family is shown. *TbRND*, *T. brucei* EAN77178; *TbRrp6*, *T. brucei* CAC39261; *ScRrp6*, *Saccharomyces cerevisiae* NP_014643; *EcRNase D*, *E. coli* NP_416318. *Hatched*, PF01612, 3′-5′ exoribonuclease domain; *grid pattern*, PF00570, HRDC domain; *white*, PF00098, CCHC zinc finger; *black with dots*, PF08066, PMC2NT domain found in some exosome components; *black*, RNase D domain (expanded directly below to show sequence homology). *C*, mitochondrial enrichment of TbRND is shown. TbRND-MHT was detected by anti-myc immunoblot of protein from total cells before (−) and after (+) tetracycline induction of TbRND-MHT expression and of mitochondrial extract following induction (*Mt*). Eight μg of protein was loaded in each lane. *TbRGG2*, mitochondrial marker; *HSP70*, cytoplasmic marker. *D*, immunofluorescent co-localization of TbRND-MHT with Mitotracker Red CMXRos (*Mito*) is shown. *DIC*, differential interference contrast. *E*, immunoblot detection of TbRND in crude protein extracts from 6×10^6 BF single marker or PF 29-13 cells is shown. MRP2 is a control for a constitutively expressed protein.

sor mass tolerance of 10 ppm and high correlation score (Xcorr) cut-offs; additional criteria are that peptide and protein probability must be 95 and 99.9% or higher, and the false discovery rate must be lower than 0.1% as determined by decoy data base search. Finally, two unique peptides must be identified for each protein. Glycerol gradient analysis of mitochondrial extracts was described previously (67). Ten μl from each fraction was analyzed by immunoblotting for TbRND.

RESULTS

The RNase D Family Protein TbRND Is Mitochondrial and Expressed in PF Cells—In an effort to identify exoribonucleases responsible for mRNA decay in *T. brucei* mitochondria, we performed a bioinformatic analysis. We first utilized degenerate motifs for various exoribonuclease classes (21) to interrogate the *T. brucei* genome data base. Of the positive hits that were potentially mitochondrial based on putative N-terminal targeting sequences, we identified the RNA editing exoribonucleases KREX1 and KREX2 (55) and the previously studied TbDSS-1 (57, 59). In addition, we identified Tb09.211.3670 as a potential mitochondrial exoribonuclease when *E. coli* RNase D was utilized as the query sequence for BLAST. We thereby termed this putative mitochondrial exoribonuclease, TbRND. TbRND is highly conserved among kinetoplastid parasites, with homologues in *T. cruzi* and *L. major* displaying 75 and 66% amino acid identity to TbRND, respectively.

TbRND possesses a 176-amino acid 3′-5′ exoribonuclease domain common to the DEDD family of exoribonucleases and an 18-amino acid sequence with very high sequence similarity to a motif specific to the RNase D subfamily (21) (Figs. 1, *A* and *B*). This subfamily includes both bacterial RNase D, a distributive exoribonuclease that acts on tRNAs, 5 SRNA, and other small RNAs *in vitro* (78), and eukaryotic Rrp6, a nuclear component of the exosome that can also be cytosolic and function independent of the exosome (79–82). The only other trypanosome RND family protein identifiable in the sequence databases is the Rrp6 homologue, which has been experimentally determined to be nuclear and cytosolic (83). The exoribonuclease domain of TbRND shares 24% identity and 41% similarity with that of *E. coli* RNase D. However, TbRND differs substantially from all other RND family members at its C terminus. Both RNase D and Rrp6 possess a C-terminal HRDC (helicase and RNase D C-terminal) domain (Fig. 1*B*). Structural analysis as well as the ability of all HRDC-containing proteins to associate with nucleic acids suggests that the RNase D HRDC domain is involved in substrate binding (78). In contrast, TbRND possesses a CCHC zinc finger domain at its C terminus, a motif unique among proteins of known exoribonuclease families (Figs. 1, *A* and *B*). These domains, found in retroviral nucleocapsid proteins and eukaryotic gene regulatory proteins, specifically bind RNA and single-stranded DNA (84–88), suggesting that the zinc finger in TbRND may substitute for the HRDC domain with regard to substrate recognition. This novel domain structure and the conservation of TbRND among kinetoplastids suggest that TbRND may recognize kinetoplastid-specific RNA targets.

In keeping with the predicted mitochondrial targeting sequence present at the N terminus of TbRND (89), a comprehensive mass spectrometric analysis of the *T. brucei* proteome assigned TbRND a mitochondrial subcellular localization with three unique TbRND peptides detected in a mitochondria-enriched sample and no peptides detected in a total cellular protein sample (90). Because neither RND family nor CCHC domain-containing proteins have been previously reported to be mitochondrial, we wanted to verify this localization. To this end, we generated a *T. brucei* cell line inducibly expressing TbRND fused to a C-terminal Myc/His/TAP (MHT) tag. Anti-myc immunoblot analysis of whole cell and mitochondrial extracts from this cell line demonstrated that TbRND is highly enriched in the mitochondrial fraction (Fig. 1*C*). Furthermore, TbRND-MHT co-localizes with MitoTracker Red CMXRos in the typical reticulated pattern of trypanosome mitochondrial staining in indirect immunofluorescence experiments, confirming the *in silico* prediction and the proteomic analysis (Fig. 1*D*). Thus, TbRND is mitochondrially localized.

Trypanosomes undergo extensive alterations in mitochondrial gene expression during life cycle transitions, resulting in highly altered mitochondrial function. Because the stability of specific RNAs is likely regulated developmentally (27, 30–33), TbRND levels may also differ between life cycle stages. To determine whether this is the case, TbRND expression was analyzed by immunoblot with anti-TbRND antisera in the two prolific life cycle stages grown in the laboratory; that is, the insect midgut PF and the mammalian BF, with the constitutively expressed protein MRP2 as a loading control (91). Although TbRND was easily observed in the PF cells, we were unable to

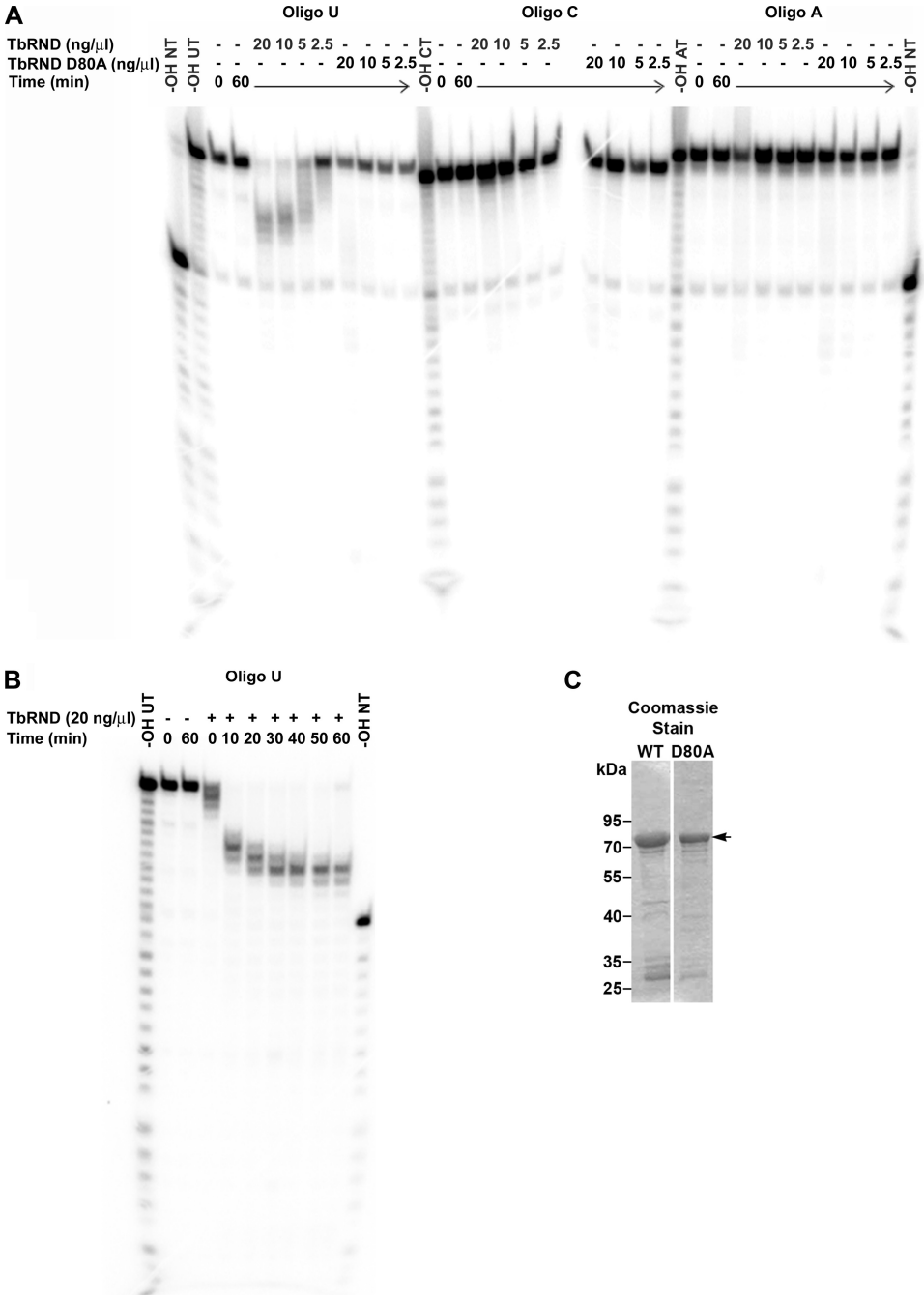

FIGURE 2. **TbRND activity.** PAGE analysis of reaction products after digestion of substrates by recombinant wild type or mutant (D80A) TbRND is shown. *A*, nucleotide specificity is shown. Substrates are 30-mer oligoribonucleotides, of which the 3′-most residues are either U_{12}, C_{12}, or A_{12} (oligo U, C, or A) (51). *-OH NT* and *-OH UT*, *-OH CT*, or *-OH AT*, alkaline hydrolysis ladder from the 18-mer oligo lacking the tail (*NT*) or possessing the U_{12}, C_{12}, or A_{12} tail. *B*, time course is shown. The 30-mer oligoribonucleotide ending in U_{12} was digested by 20 ng/μl enzyme for the indicated amounts of time. *C*, shown is a Coomassie-stained SDS-PAGE gel of purified recombinant TbRND proteins used in the assays in this figure and in Fig. 3. The *arrow* indicates the position of the full-length proteins.

detect its presence in the BF cells despite repeated attempts (Fig. 1*E*). Although we cannot rule out expression in the BF at a level undetectable by our antibody, our data clearly indicate that expression of TbRND is highly up-regulated in the PF life cycle stage.

TbRND Is a U-specific 3′-5′ Exoribonuclease—To determine whether TbRND is an exoribonuclease as its DEDD domain suggests, we purified recombinant TbRND and performed *in vitro* RNA degradation assays. The complete TbRND ORF was expressed in *E. coli* with an N-terminal GST/His_6 tag and purified by sequential cobalt and glutathione affinity chromatography (Fig. 2*C*). We also expressed and similarly purified a mutant protein, TbRND-D80A, predicted to be inactive based on the role of this residue in metal binding (78) and on a previous study of Rrp6 mutants (92) (Figs. 1*A* and 2*C*) for use as a negative control. Upon SDS-PAGE analysis of the recombinant proteins, we noted that the Coomassie-stained peptides observed below the full-length product displayed a similar banding pattern as the recombinant protein detected by TbRND immunoblot (supplemental Fig. 1), indicating that these lower bands are pri-

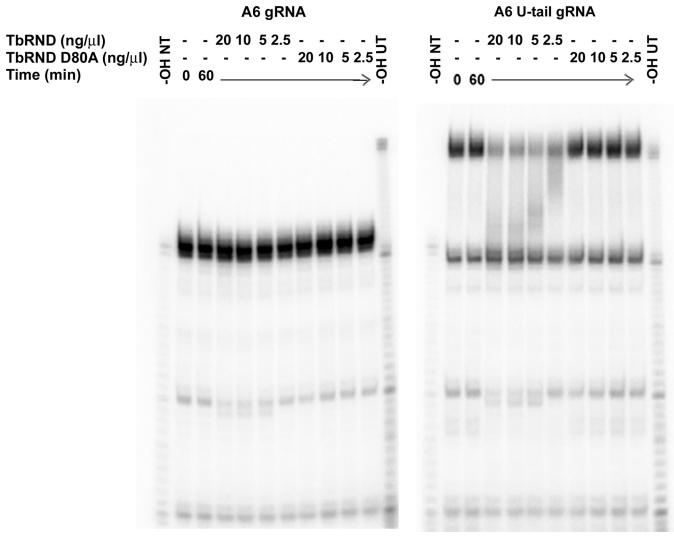

FIGURE 3. **TbRND digestion of gRNAs with or without oligo(U) tails.** Shown in a PAGE analysis of reaction products after digestion of gA6[14] (75, 95) with or without a 17-nt oligo(U) tail by recombinant wild type or mutant (D80A) TbRND. Other symbols are as in Fig. 2.

marily degradation products. We incubated increasing amounts of TbRND and TbRND-D80A with 5′-radiolabeled 30-mer oligoribonucleotide substrates ending in A_{12}, C_{12}, or U_{12} for 60 min (51). Oligomers ending in A_{12} and U_{12} have 3′ ends consistent with non-encoded sequences found on 3′ ends of *T. brucei* mitochondrial RNAs, whereas the substrate ending in C_{12} does not. Reaction products were resolved on denaturing polyacrylamide gels (Fig. 2*A*). Surprisingly, unlike RNase D, with its inability to degrade homopolymers (23), or Rrp6, with its often oligoadenylated substrates (79, 93, 94), TbRND was active primarily on the uridylated oligonucleotide. The lack of activity of TbRND-D80A demonstrated that exoribonuclease activity is inherent to TbRND and not due to contamination of the preparation by an *E. coli* exoribonuclease. Because substrates were 5′-labeled and trimming of the substrates was evident, this indicates a 3′ to 5′ progression of the enzyme. A time course analysis of TbRND activity shows that the oligonucleotide ending in U_{12} was progressively trimmed for the first 30 min, after which the activity appeared to stall three to four nucleotides before the heteropolymeric region of the substrate (Fig. 2*B*). The appearance and subsequent disappearance of intermediate-sized RNAs during the early time points defines them as reaction intermediates. The inability of TbRND to degrade the final portion of the uridine oligomeric region was consistent among experiments. From these data, we conclude that TbRND is a 3′ to 5′, U-specific exoribonuclease.

To determine whether TbRND can utilize a mitochondrial RNA as its substrate, we performed the same assay using an *in vitro* transcribed 5′ end-labeled mitochondrial gRNA as substrate. Because gRNAs possess non-encoded oligo(U) tails, they represent a potential cellular target of TbRND. We incubated increasing amounts of recombinant TbRND with 5′ end-labeled gA6[14] (75, 95) gRNA either possessing an oligo$(U)_{17}$ tail or lacking an oligo(U) tail for 60 min. Fig. 3 shows that TbRND was able to trim the oligo(U) tail of the gRNA but could not utilize the untailed substrate. Thus, TbRND has the potential to act on gRNAs *in vivo*.

TbRND Depletion Affects gRNA Oligo(U) Tail Length—With its identity as a 3′ to 5′ exoribonuclease confirmed *in vitro*, we next analyzed the role of TbRND in the mitochondria of PF *T. brucei*. To this end, we generated clonal cell lines expressing tet-regulated RNA interference against TbRND. We analyzed multiple clones, all of which exhibited TbRND mRNA depletion by qRT-PCR to approximately the same level. In the clone utilized in this study, TbRND mRNA levels were reduced to 0.32 ± 0.01 ($n = 9$) of normal levels (not shown).

Because TbRND is a mitochondrial exoribonuclease, TbRND-depleted cells may exhibit an over-accumulation of certain mitochondrial RNAs resulting from their enhanced stability in the absence of this exoribonuclease activity. To identify any stabilized RNAs, we performed qRT-PCR on a panel of mitochondrial RNAs that included pre-edited and edited A6, CO2, CO3, CYb, MURF2, RPS12, and ND8 mRNAs, the never-edited CO1, MURF1, ND1, and ND4 mRNAs, and the 9 S and 12 S rRNAs. In addition, qRT-PCR primers bridging the adjacent genes 9 S and ND8, CYb and A6, and RPS12 and ND5 were used to amplify preprocessed RNAs. Analyses were performed in triplicate from two biological replicates; however, none of these RNAs was significantly stabilized in TbRND-depleted cells (not shown and Fig. 4*C*). Limited circular RT-PCR assays also did not reveal any substantial alterations in lengths or A/U ratios of mRNA 3′ tails (not shown). We also analyzed the abundance of three tRNAs, Ile(UAU), Cys(GCA), and Gln(UUG), by Northern blot in RNA samples prepared from mitochondria (96). Depletion of TbRND had no effect on the levels or sizes of these tRNAs (not shown), indicating that TbRND is not involved in the maintenance of this RNA species.

Because TbRND preferentially degrades U homopolymers and gRNA oligo(U) tails serve as an *in vitro* substrate (Figs. 2 and 3), we next analyzed the effect of TbRND depletion on the abundance and size of gRNAs. If gRNAs are *in vivo* TbRND substrates, depletion of TbRND would likely result in longer oligo(U) tails and, possibly, increased gRNA levels. Because there are at least 1200 different classes of gRNAs, it is not feasible to examine a large proportion of specific gRNAs by qRT-PCR or RNA blot. However, the total gRNA population can be easily assessed by direct guanylyltransferase labeling of total cellular RNA (70, 71). To examine the effect of TbRND depletion on gRNAs *in vivo*, we labeled total RNA from uninduced and induced TbRND RNAi cells using [α-^{32}P]GTP and guanylyltransferase. We then visualized labeled gRNAs, which appear as a ladder of transcripts migrating between 55–70 nt, on a high resolution polyacrylamide gel (Fig. 4*B*). We normalized the total signal intensities from bands in this region to the labeled cytosolic primary transcript and averaged the values from duplicate experiments. The signal from TbRND RNAi cells was 1.0 ± 0.13 that of uninduced cells, demonstrating that the overall quantity of gRNAs does not change significantly upon TbRND depletion. However, a qualitative analysis of these gels shows that the gRNA population from TbRND-depleted cells is reproducibly 2–3 nt longer as a result of TbRND depletion (Figs. 4, *A* and *B*). This suggests that gRNA oligo(U) tail length is at least partly controlled by TbRND. To determine whether this effect is specific to gRNAs or common to all uridylated RNAs, we next analyzed the 3′ ends of 9 S and 12 S rRNAs,

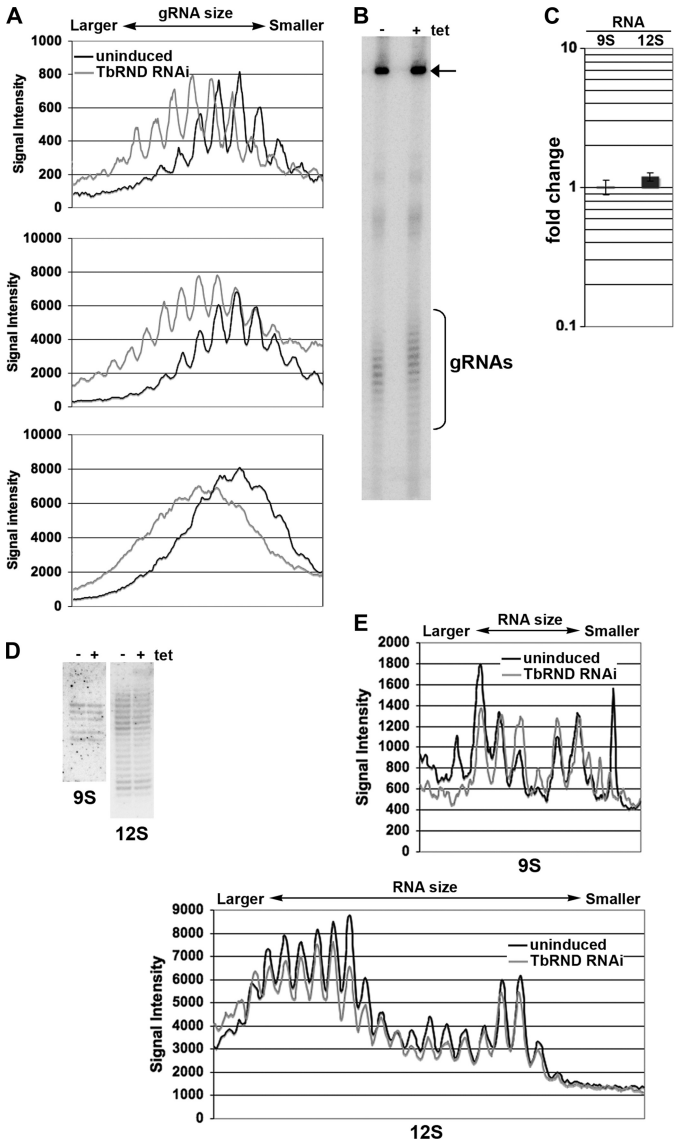

FIGURE 4. **Nucleotide length of the gRNA population increases upon TbRND depletion.** *A*, quantitation of band intensity from PAGE of RNAs labeled with guanylytransferase and [α-^{32}P]GTP along the length of a gel (*x* axis) in the gel region where gRNAs migrate. Each graph depicts data from an independent RNAi induction and RNA collection. *B*, shown is representative polyacrylamide electrophoresis gel from *A* depicting gRNAs from TbRND RNAi cells grown in the absence (−) or presence (+) of tetracycline. The *arrow* indicates cytosolic RNA used as a loading control. *C*, shown is the ratio of 18 S-normalized rRNA abundances from TbRND RNAi-induced cells to uninduced cells, with a value of 1 indicating equal abundance under both conditions, as determined by quantitative RT-PCR. RNA levels represent the mean and S.E. of three determinations. *D*, Northern blot analysis of 9 S or 12 S rRNA after RNase H cleavage of the 3′ end of the rRNA from the rest of the transcript is shown. *E*, quantitation of rRNA band intensity along the length of the blot (*x* axis) is shown.

whose abundance did not change upon TbRND depletion in qRT-PCR assays as shown in Fig. 4*C*. To accurately measure changes in rRNA oligo(U) tail length, we first performed RNase H cleavage using an antisense oligonucleotide to a region of each rRNA near its 3′ end to generate free 3′ ends in the 60–80-nt size range. When the RNA was electrophoresed on a 10% polyacrylamide gel, these 3′ rRNA fragments migrated in a range in which RNAs differing in size by a single nucleotide was distinguishable. Qualitative northern blotting to detect the cleaved 3′ rRNA fragments revealed no significant differences in the sizes of the rRNA populations between RNA from uninduced and induced TbRND RNAi cells (Figs. 4, *D* and *E*). From these data, we conclude that TbRND specifically affects the lengths of gRNA oligo(U) tails *in vivo*.

TbRND-MHT Overexpression Inhibits Growth and Depletes Full-length gRNAs—To further probe the *in vivo* function of TbRND in mitochondrial RNA metabolism, we analyzed the effects of TbRND overexpression on mitochondrial RNA populations by comparing cells before and after the induction of TbRND-MHT. Immunoblot analysis with anti-TbRND antibodies demonstrates that the tagged protein is expressed at approximately three to four times the level of the native protein upon tet induction (Fig. 5*A*). To determine whether any observed effects of overexpression required the catalytic activity of TbRND, we also generated a cell line expressing TbRND-MHT-D80A, which when induced under the same conditions, expressed the mutant protein at a level >10-fold greater than native levels. Immunofluorescence microscopy verified that TbRND-MHT-D80A localized to the mitochondria as expected (not shown). Before analysis of mitochondrial RNA populations in TbRND overexpressing cells, it was first essential to confirm that TbRND with this C-terminal extension is active. To this end, we purified tagged proteins from the TbRND-MHT- and TbRND-MHT-D80A-expressing cells by TAP, resulting in purified TbRND with Myc, His, and calmodulin binding domain tags (TbRND-MHC). The purified preparations contained single bands of expected size observable on a silver-stained SDS-PAGE gel (Fig. 5*B*). We then assessed the activity of these proteins in an *in vitro* degradation assay as shown in Fig. 5*C* using gRNAs with or without an oligo(U) tail as substrates. The activities of the trypanosome-derived enzymes mimicked those of the bacterially derived proteins. That is, the wild type enzyme exhibited activity toward uridylated, but not non-uridlyated, gRNA, whereas the D80A mutant was inactive toward both substrates. We note that 20-fold less *T. brucei*-derived wild type protein was needed to achieve the same degree of degradation as bacterially expressed protein, possibly because a high percentage of our *E. coli*-derived TbRND was not properly folded or modified. Thus, the *T. brucei* TbRND-MHT cell line expresses active TbRND at higher than normal levels and is suitable for studying the effects of overexpression on mitochondrial RNA metabolism.

Overexpression of active TbRND-MHT resulted in a profound growth defect (Fig. 6*A*, *top graph*), suggesting that TbRND plays an important role in mitochondrial RNA metabolism. In contrast, when we overexpressed the catalytically inactive TbRND-MHT-D80A (Fig. 6*A*, *bottom graph*), the effect on growth was minimal, indicating that the catalytic activity of TbRND is necessary for the observed growth effects. Because we detected an effect of TbRND depletion on gRNAs, we first examined the result of TbRND overexpression on this RNA population. Guanylyltransferase labeling demonstrated that the total gRNA population was significantly reduced upon expression of the wild type (0.66 ± 0.14 compared with uninduced control, $n = 5$) but not the D80A mutant TbRND-MHT (1.3 ± 0.33 compared with uninduced control, $n = 3$; Fig. 6*B*), strengthening the argument that TbRND may be responsible

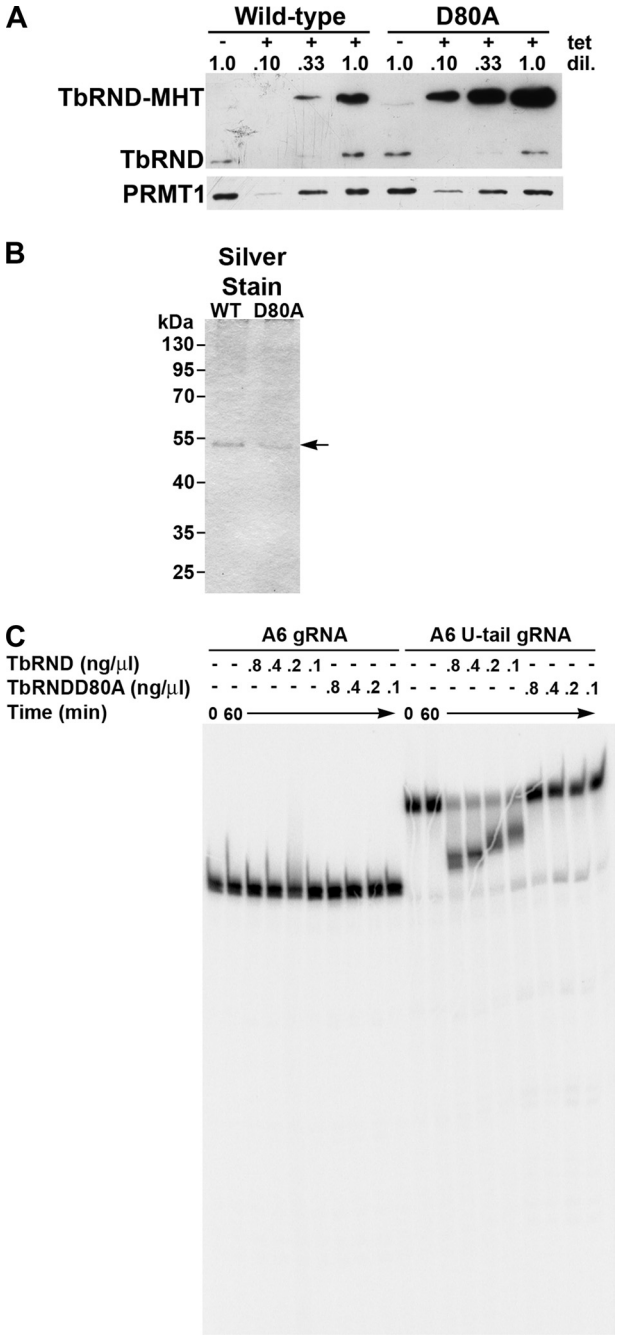

FIGURE 5. **Tetracycline-regulateable expression of active tagged TbRND in PF *T. brucei*.** *A*, an immunoblot with anti-TbRND antibodies shows the level of expression of wild type and mutant (D80A) TbRND-MHT at 48 h post-induction relative to native TbRND. Dilution (*dil*) 1.0 represents crude extract from 6×10^6 cells. PRMT1 is a loading control. *B*, shown is a silver-stained SDS-PAGE gel of purified wild type and D80A mutant TbRND-MHC proteins, with their position indicated by an *arrow*. *C*, shown is a PAGE analysis of reaction products after digestion of gA6[14] with (79 nt) and without (62 nt) an oligo$(U)_{17}$ tail by wild type and D80A mutant TbRND-MHC shown in *B*.

for some aspect of gRNA metabolism. To assess whether the observed gRNA depletion led to defects in RNA editing, we performed qRT-PCR analysis of pre-edited and edited mRNAs. Indeed, editing of almost all RNAs examined was strongly decreased (Fig. 6*C*). The abundance of extensively edited RNAs, which require many gRNAs to achieve complete editing, ranged from 10 to 40% that of normal levels. Depletion was less severe, to about 50–60% that of normal levels, in two transcripts that are only minimally edited and, thus, require only a few gRNAs. In all instances we observed an increased accumulation of pre-edited RNAs, which is expected if editing is compromised at its initial step as in the absence of abundant gRNA. Interestingly, editing of CO2 RNA was completely unaffected by TbRND overexpression. CO2 RNA is minimally edited; however, its editing is guided not by a typical *trans*-acting oligo(U)-tailed gRNA but by a *cis*-acting gRNA encoded at the mRNA 3′ end. The absence of an effect on CO2 RNA editing implies that the inhibition of editing of other RNAs is not due to a defect in editosome function but rather in the *trans*-acting gRNAs. The six never-edited transcripts remained unaffected by high levels of TbRND. Finally, we observed a very modest accumulation (about 150% of normal levels) of CO2 pre-edited RNA as well as pre-processed RNA species that include a pre-edited mRNA. In contrast, when RNA from cells expressing catalytically inactive TbRND-D80A-MHT was used for analysis of select edited transcripts A6, CO3, CO2, and CYb, these editing-related changes in abundance were not observed (Fig. 6*D*). From these data, we conclude that gRNA is an *in vivo* TbRND substrate, and through modulation of gRNA abundance, TbRND activity can indirectly affect RNA editing.

TbRND Is Not Part of a High Molecular Weight Complex but Associates with MRB1 Complex Components—Many exoribonucleases, including the RND family member Rrp6, exist in macromolecular complexes with other RNA binding proteins, helicases, and exoribonucleases (16, 58, 97–100). TAP purification of TbRND-MHT resulted in a protein preparation with no other proteins observable by silver stain (Fig. 5*B*). However, the process of purification may have disrupted interactions it would normally have with other proteins, or the higher level of expression of tagged TbRND may have skewed the cellular ratio of TbRND with its normal binding partners. To determine whether TbRND is normally part of a protein complex, we fractionated mitochondrial extract from wild type cells on a 10–30% glycerol gradient and probed by immunoblot for the presence of endogenous TbRND (Fig. 7*A*). We observed TbRND exclusively in fractions 1 and 2, indicating that TbRND is not a stable component of a large complex able to withstand glycerol gradient sedimentation.

The absence of a readily observable stable macromolecular complex containing TbRND does not rule out more transient and/or substoichiometric associations. Furthermore, in the gradient fractionation range where TbRND is observed, very small complexes would be indistinguishable from TbRND monomers. To address the possibility of these types of associations, we performed LC-MS/MS analysis on a TbRND-MHC preparation in an effort to identify interacting partners. As expected, by far the most peptides, 31 unique peptides in total, were products of digestion of TbRND or its tag. Notably, among the other products of trypsin digestion present in lower abundance, we identified multiple peptides from four members the mitochondrial RNA binding complex 1 (MRB1). The MRB1 complex appears to have multiple roles in mitochondrial RNA metabolism, including functions in gRNA stability, mRNA stability, and RNA editing (60, 61, 66, 73, 101, 102). Different members of this complex have co-purified depending on which

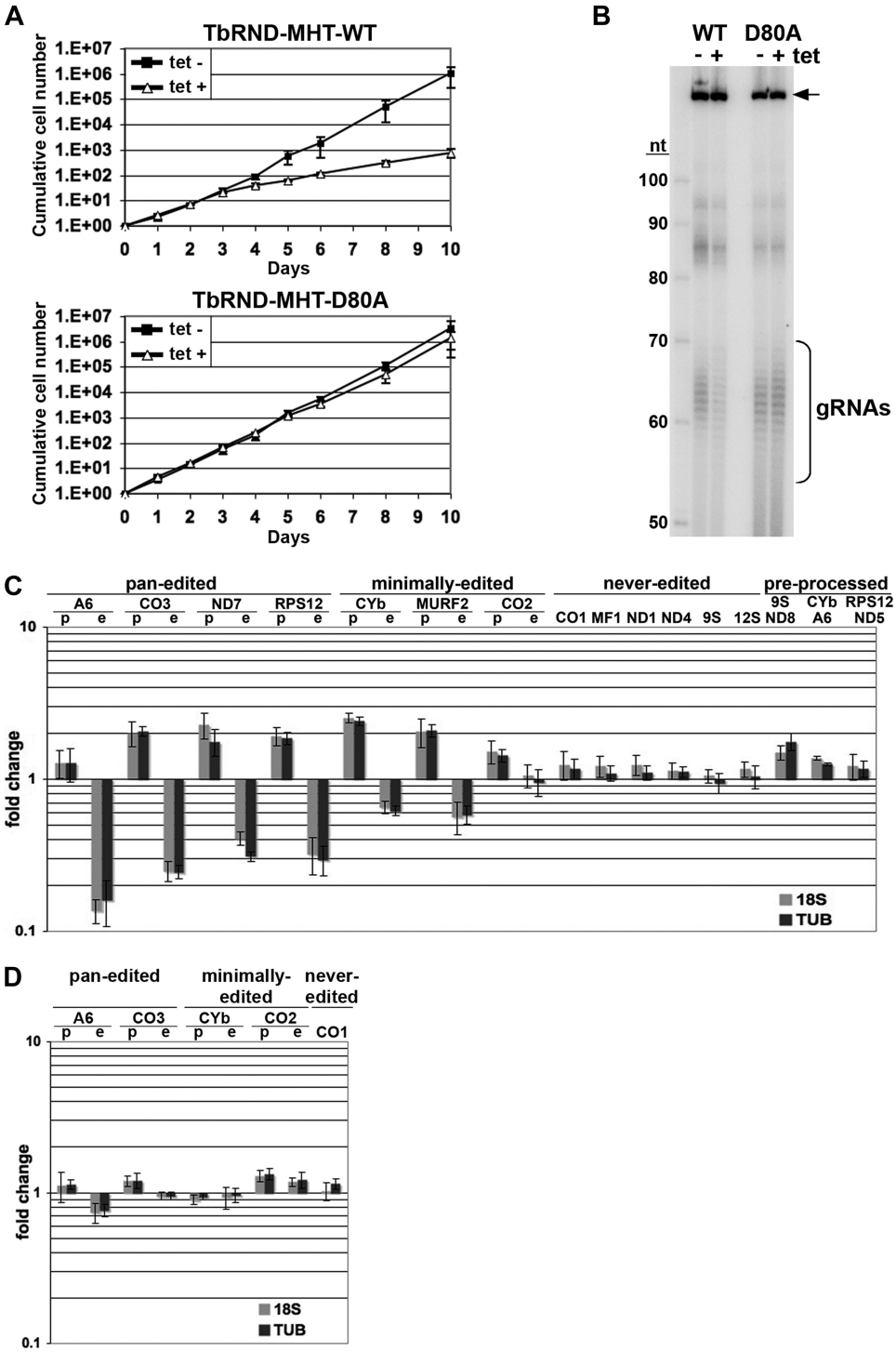

FIGURE 6. **Effects of TbRND overexpression.** *A*, shown is mean growth (±S.D.; $n = 3$) of PF *T. brucei* with and without tet-regulated induction of wild type (*WT*) and D80A mutant TbRND-MHT expression. *B*, shown is a PAGE analysis of total cellular RNA labeled with guanylytransferase and [α-^{32}P]GTP before and after a 2-day induction of WT or D80A mutant TbRND-MHT. The *arrow* indicates cytosolic RNA used as a loading control. *C*, shown is the Ratio of mitochondrial RNA abundances from TbRND-MHT-overexpressing cells relative to those in uninduced cells (-fold change) with a value of 1 indicating equal abundance under both conditions, as determined by quantitative RT-PCR analysis with normalization to cytoplasmic 18 S rRNA and β-tubulin (*TUB*) mRNA. RNA levels represent the mean and S.E. of 5–6 determinations. *p*, pre-edited; *e*, edited. *D*, quantitative RT-PCR analysis of select mitochondrial RNAs from TbRND-D80A-MHT mutant expressing cells is shown.

component was tagged for purification and in which laboratory the study was performed (61, 66, 101). In our TbRND-MHC preparation, we detected GAP1 and GAP2, which comprise a 200-kDa heterotetramer (GAP1/2) and are of interest because they bind and stabilize gRNAs (39, 60, 61). In addition, we identified TbRGG2, a protein that affects editing of pan-edited RNAs at least partially by affecting gRNA utilization (66, 67) and Tb927.4.4160, whose function is unknown. To confirm the LC-MS/MS results and determine whether additional members of the MRB1 complex associate with TbRND, we per-

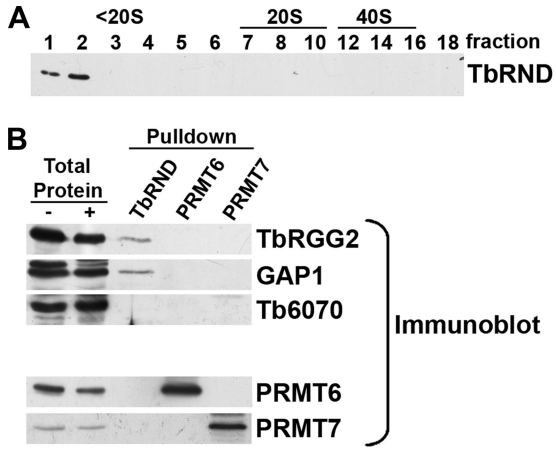

FIGURE 7. **Macromolecular associations with TbRND.** *A*, mitochondrial extracts from PF 29-13 cells were fractionated on a 10–30% glycerol gradient, and fractions were immunoblotted using anti-TbRND antibodies. *B*, immunoblot analysis of a purified TbRND-MHC protein preparation is shown. PRMT6-MHC and PRMT7-MHC serve as nonspecific binding controls. *Total protein* represents total extracts of TbRND-MHT cells grown in the absence (−, lacking TbRND-MHT) or presence (+, expressing TbRND-MHT) of tetracycline.

formed immunoblot analysis on the TbRND-MHC protein preparation with available antibodies (Fig. 7*B*). TAP preparations of two unrelated proteins, TbPRMT6 and TbPRMT7, were included as negative controls for nonspecific binding. TbRGG2 and GAP1 were readily detected in TbRND purifications but not in control purifications, confirming the LC-MS/MS results. In contrast, another member of the complex found in one MRB1 pulldown assay, Tb927.2.6070 (101), was not present. These data suggest that TbRND does not associate with the MRB1 complex in one of its larger forms, but rather, TbRND may interact with individual complex components or small subcomplexes, consistent with the apparent small size of TbRND on glycerol gradients (Fig. 7*A*). Finally, in an effort to clarify the TbRND-GAP1/2 relationship, we generated cells expressing HA-tagged GAP1 and performed co-immunoprecipitation assays (not shown). However, we did not detect TbRND in GAP1-HA precipitates. Collectively, these data suggest a scenario whereby a small percentage of purified TbRND-MHC is bound to gRNAs that are also associated with the MRB1 complex or subcomplexes thereof, consistent with a role for TbRND in gRNA metabolism.

DISCUSSION

Here we show that TbRND, the first reported organellar member of the RNase D family, is a U-specific 3′-5′ exoribonuclease. Oligouridylated gRNAs that are *trans*-acting factors in kinetoplastid RNA editing act as substrates for TbRND both *in vitro* and *in vivo*. TbRND resembles other members of the RNase D family in that one of its *in vivo* targets is a small noncoding RNA. However, gRNAs are specific to kinetoplastid protozoa, consistent with the unusual domain structure of TbRND in which a CCHC zinc finger replaces the HRDC substrate binding domain of other RNase D family enzymes. We speculate that substrate binding by the CCHC zinc finger may confer oligo(U) specificity, as this is what sets TbRND apart from the other RNase D-like enzymes that do not degrade U-tailed RNAs. To our knowledge, no other exoribonucleases containing such a domain have been reported in any organism. TbRND is mitochondrially localized, as demonstrated by immunofluorescence and immunoblotting, consistent with its ability to degrade gRNA oligo(U) tails. Expression of TbRND is developmentally regulated during the *T. brucei* life cycle, being detectable only in the PF stage.

Several lines of evidence indicate that TbRND plays a role in gRNA metabolism *in vivo*. First, upon RNAi-mediated depletion of TbRND, the total gRNA population is extended by 2–3 nt. Second, overexpression of TbRND leads to a significant depletion of the total gRNA population, which is reflected in a consequent inhibition of RNA editing. TbRND exhibits specificity for gRNAs *in vivo* as rRNAs, which also possess oligo(U) tails, are unaffected by TbRND depletion or overexpression. Finally, TbRND pulldown assays contain a subset of proteins from the MRB1 complex, notably GAP1/2 and TbRGG2, which are thought to function in gRNA stabilization and utilization, respectively (60, 61, 67). Additional reported members of the MRB1 complex were absent from TbRND pulldown assays, indicating the specificity of the TbRND interaction with proteins involved in gRNA maintenance and usage. The 2–3-nt extensions of gRNAs observed in TbRND-depleted cells imply that the enzyme constitutively accesses and nibbles at gRNA 3′ ends. The observation that TbRND can degrade oligo(U) tails longer than 2–3 nt *in vitro* suggests that TbRND is actively prevented from degrading further into gRNA oligo(U) tails *in vivo*. One possibility is that GAP1/2 stabilizes gRNAs against TbRND-mediated decay by blocking TbRND progression. Although GAP1/2 is capable of binding the encoded portion of gRNAs (39), it may physically occlude access of TbRND to the majority of the oligo(U) tail. If this scenario were correct, one would predict that gRNAs, which decay in GAP1/2 knockdowns (60, 61), would remain stable if GAP1/2 and TbRND were simultaneously knocked down. We did not observe stabilization of gRNAs under these conditions[3]; however, we cannot rule out that the remaining TbRND is still sufficient for gRNA decay in the absence of GAP1/2. Alternatively, TbRND progression may be impeded *in vivo* by other gRNA binding proteins or intermolecular RNA-RNA interactions.

In vitro, TbRND is completely unable to degrade an RNA lacking an oligo(U) tail. On oligo(U)-tailed RNAs, TbRND efficiently degrades the oligo(U) tail to nt −3 or −4 before the start of the heteropolymeric region of the RNA. A similar activity has been reported for the mammalian poly(A)-specific ribonuclease, an adenine-preferring exoribonuclease that also binds and cleaves poly(U) and belongs to the same exoribonuclease superfamily as TbRND (103). The authors showed that when A_{20} or U_{20} substrates were used, the reaction proceeds through multiple kinetically distinct reaction phases including very retarded kinetics once the homopolymer had shortened to A_4 or U_5. Poly(A)-specific ribonuclease was hypothesized to degrade long substrates better than short substrates because the longer substrate could bind to regions outside of the active site (103). Future experiments defining the precise RNA binding sites of TbRND and their contribution to TbRND interaction with dif-

[3] S. L. Zimmer and L. K. Read, unpublished observations.

fering length U-tails will provide insight into whether poly(A)-specific ribonuclease and TbRND exhibit similar mechanisms in this regard. Interestingly, we previously reported that in mitochondrial extracts, gRNAs undergo biphasic decay, entailing rapid deuridylation followed by a slower decay of the encoded portion of the gRNA (104). Our data suggest that TbRND may function in the first step of this decay process. Based on results from cells in which TbRND is overexpressed, removal of the oligo(U)-tail by TbRND appears to leave the remainder of the gRNA susceptible to decay, likely by another exoribonuclease. Conversely, *in vivo* gRNA decay studies in cells depleted of RET1, the TUTase that adds oligo(U)-tails to gRNAs, suggested that removal of the oligo(U) tail does not lead to gRNA destabilization (39). Likely the conflicting results are due to the very different cell lines examined. Additional experiments are necessary to clarify the role of gRNA oligo(U) tails in gRNA stability.

Several questions regarding the *in vivo* role(s) of TbRND remain. For example, when in the life cycle of a gRNA does it become subject to TbRND-mediated decay? Although gRNAs must be degraded at some point in their life cycles, almost nothing is known about the timing of this process. Early studies of a limited number of gRNAs suggest that their abundance does not change in parallel with their developmentally regulated cognate mRNAs (33, 95, 105). Rather, gRNAs generally accumulated in an inverse relationship to their cognate edited RNAs, implying that gRNAs are degraded as a consequence of the editing process (105). Thus, one potential role for TbRND is in a basal-level editing-linked gRNA decay pathway. This raises a second question as to why TbRND appears to be absent or in very low abundance in BF. There may be additional or redundant enzymes that perform this function in BF. Alternatively, a low level of TbRND may suffice in BF mitochondria, which require editing (106) but whose function is down-regulated compared with PF. It is of interest in this regard that TbRGG2, which is involved in gRNA utilization and is essential in BF, is nevertheless present at 10-fold lower levels in BF than PF (67). Future studies will be aimed at determining the precise timing of TbRND action in gRNA metabolism and understanding the role of its novel zinc finger domain.

Acknowledgments—We thank Danielle Tomasello and Kurtis Downey for technical assistance, members of the Read laboratory for useful discussions, and Dr. Michelle Ammerman for critical reading of the manuscript. We are also grateful to Dr. Arthur Gunzl for providing the GAP1-HA construct, Dr. Jay Bangs for anti-Hsp70 antibody, Drs. Juan Alfonzo and Andre Schneider for advice on mitochondrial tRNA blots, and Dr. Jose García Salcedo for advice on staining cells in suspension.

REFERENCES

1. Keene, J. D. (2010) *Endocrinology* **151,** 1391–1397
2. Belostotsky, D. (2009) *Curr. Opin. Cell Biol.* **21,** 352–358
3. Evguenieva-Hackenberg, E., and Klug, G. (2009) *Prog. Mol. Biol. Transl. Sci.* **85,** 275–317
4. Haile, S., and Papadopoulou, B. (2007) *Curr. Opin. Microbiol.* **10,** 569–577
5. Lange, H., Sement, F. M., Canaday, J., and Gagliardi, D. (2009) *Trends Plant Sci.* **14,** 497–504
6. Lorković, Z. J. (2009) *Trends Plant Sci.* **14,** 229–236
7. Picard, F., Dressaire, C., Girbal, L., and Cocaign-Bousquet, M. (2009) *C. R. Biol.* **332,** 958–973
8. Anderson, J. T., and Wang, X. (2009) *Crit. Rev. Biochem. Mol. Biol.* **44,** 16–24
9. Borowski, L. S., Szczesny, R. J., Brzezniak, L. K., and Stepien, P. P. (2010) *Biochim. Biophys. Acta* **1797,** 1066–1070
10. Cristodero, M., and Clayton, C. E. (2007) *Nucleic Acids Res.* **35,** 7023–7030
11. Etheridge, R. D., Aphasizheva, I., Gershon, P. D., and Aphasizhev, R. (2008) *EMBO J.* **27,** 1596–1608
12. Moore, M. J., and Proudfoot, N. J. (2009) *Cell* **136,** 688–700
13. Portnoy, V., and Schuster, G. (2006) *Nucleic Acids Res.* **34,** 5923–5931
14. Régnier, P., and Hajnsdorf, E. (2009) *Prog. Mol. Biol. Transl. Sci.* **85,** 137–185
15. Ibrahim, F., Rymarquis, L. A., Kim, E. J., Becker, J., Balassa, E., Green, P. J., and Cerutti, H. (2010) *Proc. Natl. Acad. Sci. U.S.A.* **107,** 3906–3911
16. Lin-Chao, S., Chiou, N. T., and Schuster, G. (2007) *J. Biomed. Sci.* **14,** 523–532
17. Mullen, T. E., and Marzluff, W. F. (2008) *Genes Dev.* **22,** 50–65
18. Ramachandran, V., and Chen, X. (2008) *Science* **321,** 1490–1492
19. Rissland, O. S., and Norbury, C. J. (2009) *Nat. Struct. Mol. Biol.* **16,** 616–623
20. Wickens, M., and Kwak, J. E. (2008) *Science* **319,** 1344–1345
21. Zuo, Y., and Deutscher, M. P. (2001) *Nucleic Acids Res.* **29,** 1017–1026
22. Li, Z., Pandit, S., and Deutscher, M. P. (1998) *Proc. Natl. Acad. Sci. U.S.A.* **95,** 2856–2861
23. Cudny, H., Zaniewski, R., and Deutscher, M. P. (1981) *J. Biol. Chem.* **256,** 5633–5637
24. Schuster, G., and Stern, D. (2009) *Prog. Mol. Biol. Transl. Sci.* **85,** 393–422
25. Stuart, K., Brun, R., Croft, S., Fairlamb, A., Gürtler, R. E., McKerrow, J., Reed, S., and Tarleton, R. (2008) *J. Clin. Invest.* **118,** 1301–1310
26. Shapiro, T. A., and Englund, P. T. (1995) *Annu. Rev. Microbiol.* **49,** 117–143
27. Feagin, J. E., Jasmer, D. P., and Stuart, K. (1985) *Nucleic Acids Res.* **13,** 4577–4596
28. Grams, J., McManus, M. T., and Hajduk, S. L. (2000) *EMBO J.* **19,** 5525–5532
29. Koslowsky, D. J., and Yahampath, G. (1997) *Mol. Biochem. Parasitol.* **90,** 81–94
30. Read, L. K., Myler, P. J., and Stuart, K. (1992) *J. Biol. Chem.* **267,** 1123–1128
31. Bhat, G. J., Souza, A. E., Feagin, J. E., and Stuart, K. (1992) *Mol. Biochem. Parasitol.* **52,** 231–240
32. Seiwert, S. D., and Stuart, K. (1994) *Science* **266,** 114–117
33. Souza, A. E., Myler, P. J., and Stuart, K. (1992) *Mol. Cell. Biol.* **12,** 2100–2107
34. Souza, A. E., Shu, H. H., Read, L. K., Myler, P. J., and Stuart, K. D. (1993) *Mol. Cell. Biol.* **13,** 6832–6840
35. Read, L. K., Stankey, K. A., Fish, W. R., Muthiani, A. M., and Stuart, K. (1994) *Mol. Biochem. Parasitol.* **68,** 297–306
36. Feagin, J. E., and Stuart, K. (1988) *Mol. Cell. Biol.* **8,** 1259–1265
37. Koslowsky, D. J., Bhat, G. J., Perrollaz, A. L., Feagin, J. E., and Stuart, K. (1990) *Cell* **62,** 901–911
38. Kao, C. Y., and Read, L. K. (2005) *Mol. Cell. Biol.* **25,** 1634–1644
39. Aphasizheva, I., and Aphasizhev, R. (2010) *Mol. Cell. Biol.* **30,** 1555–1567
40. Decker, C. J., and Sollner-Webb, B. (1990) *Cell* **61,** 1001–1011
41. Kao, C. Y., and Read, L. K. (2007) *Mol. Biochem. Parasitol.* **154,** 158–169
42. Ryan, C. M., Militello, K. T., and Read, L. K. (2003) *J. Biol. Chem.* **278,** 32753–32762
43. Militello, K. T., and Read, L. K. (1999) *Nucleic Acids Res.* **27,** 1377–1385
44. Blum, B., and Simpson, L. (1990) *Cell* **62,** 391–397
45. Koslowsky, D. J., Reifur, L., Yu, L. E., and Chen, W. (2004) *RNA Biol.* **1,** 28–34
46. Leung, S. S., and Koslowsky, D. J. (2001) *Nucleic Acids Res.* **29,** 703–709
47. Yu, L. E., and Koslowsky, D. J. (2006) *RNA* **12,** 1050–1060
48. Adler, B. K., Harris, M. E., Bertrand, K. I., and Hajduk, S. L. (1991) *Mol.*

Cell. Biol. **11,** 5878–5884
49. Kang, X., Rogers, K., Gao, G., Falick, A. M., Zhou, S., and Simpson, L. (2005) *Proc. Natl. Acad. Sci. U.S.A.* **102,** 1017–1022
50. Niemann, M., Kaibel, H., Schlüter, E., Weitzel, K., Brecht, M., and Göringer, H. U. (2009) *Nucleic Acids Res.* **37,** 1897–1906
51. Rogers, K., Gao, G., and Simpson, L. (2007) *J. Biol. Chem.* **282,** 29073–29080
52. Osato, D., Rogers, K., Guo, Q., Li, F., Richmond, G., Klug, F., and Simpson, L. (2009) *RNA* **15,** 1338–1344
53. Panigrahi, A. K., Ernst, N. L., Domingo, G. J., Fleck, M., Salavati, R., and Stuart, K. D. (2006) *RNA* **12,** 1038–1049
54. Rusché, L. N., Cruz-Reyes, J., Piller, K. J., and Sollner-Webb, B. (1997) *EMBO J.* **16,** 4069–4081
55. Schnaufer, A., Wu, M., Park, Y. J., Nakai, T., Deng, J., Proff, R., Hol, W. G., and Stuart, K. D. (2010) *J. Biol. Chem.* **285,** 5282–5295
56. Stuart, K. D., Schnaufer, A., Ernst, N. L., and Panigrahi, A. K. (2005) *Trends Biochem. Sci.* **30,** 97–105
57. Mattiacio, J. L., and Read, L. K. (2008) *Nucleic Acids Res.* **36,** 319–329
58. Mattiacio, J. L., and Read, L. K. (2009) *FEBS Lett.* **583,** 2333–2338
59. Penschow, J. L., Sleve, D. A., Ryan, C. M., and Read, L. K. (2004) *Eukaryot. Cell* **3,** 1206–1216
60. Hashimi, H., Cicová, Z., Novotná, L., Wen, Y. Z., and Lukes, J. (2009) *RNA* **15,** 588–599
61. Weng, J., Aphasizheva, I., Etheridge, R. D., Huang, L., Wang, X., Falick, A. M., and Aphasizhev, R. (2008) *Mol. Cell* **32,** 198–209
62. Jensen, B. C., Kifer, C. T., Brekken, D. L., Randall, A. C., Wang, Q., Drees, B. L., and Parsons, M. (2007) *Mol. Biochem. Parasitol.* **151,** 28–40
63. Wickstead, B., Ersfeld, K., and Gull, K. (2002) *Mol. Biochem. Parasitol.* **125,** 211–216
64. Wirtz, E., Leal, S., Ochatt, C., and Cross, G. A. (1999) *Mol. Biochem. Parasitol.* **99,** 89–101
65. Harris, M. E., Moore, D. R., and Hajduk, S. L. (1990) *J. Biol. Chem.* **265,** 11368–11376
66. Hashimi, H., Zíková, A., Panigrahi, A. K., Stuart, K. D., and Lukes, J. (2008) *RNA* **14,** 970–980
67. Fisk, J. C., Ammerman, M. L., Presnyak, V., and Read, L. K. (2008) *J. Biol. Chem.* **283,** 23016–23025
68. Fisk, J. C., Zurita-Lopez, C., Sayegh, J., Tomasello, D. L., Clarke, S. G., and Read, L. K. (2010) *Eukaryot. Cell* **9,** 866–877
69. Engstler, M., and Boshart, M. (2004) *Genes Dev.* **18,** 2798–2811
70. Hayman, M. L., and Read, L. K. (1999) *J. Biol. Chem.* **274,** 12067–12074
71. Pollard, V. W., and Hajduk, S. L. (1991) *Mol. Cell. Biol.* **11,** 1668–1675
72. Carnes, J., Trotter, J. R., Ernst, N. L., Steinberg, A., and Stuart, K. (2005) *Proc. Natl. Acad. Sci. U.S.A.* **102,** 16614–16619
73. Acestor, N., Panigrahi, A. K., Carnes, J., Zíková, A., and Stuart, K. D. (2009) *RNA* **15,** 277–286
74. Aphasizheva, I., Ringpis, G. E., Weng, J., Gershon, P. D., Lathrop, R. H., and Aphasizhev, R. (2009) *RNA* **15,** 1322–1337
75. Read, L. K., Göringer, H. U., and Stuart, K. (1994) *Mol. Cell. Biol.* **14,** 2629–2639
76. Schimanski, B., Nguyen, T. N., and Günzl, A. (2005) *Eukaryot. Cell* **4,** 1942–1950
77. Duan, X., Young, R., Straubinger, R. M., Page, B., Cao, J., Wang, H., Yu, H., Canty, J. M., and Qu, J. (2009) *J. Proteome Res.* **8,** 2838–2850
78. Zuo, Y., Wang, Y., and Malhotra, A. (2005) *Structure* **13,** 973–984
79. Callahan, K. P., and Butler, J. S. (2010) *J. Biol. Chem.* **285,** 3540–3547
80. Callahan, K. P., and Butler, J. S. (2008) *Nucleic Acids Res.* **36,** 6645–6655
81. Graham, A. C., Kiss, D. L., and Andrulis, E. D. (2006) *Mol. Biol. Cell* **17,** 1399–1409
82. Haile, S., Cristodero, M., Clayton, C., and Estévez, A. M. (2007) *Mol. Biochem. Parasitol.* **151,** 52–58
83. Haile, S., Estevez, A. M., and Clayton, C. (2003) *RNA* **9,** 1491–1501
84. Clay, N. K., and Nelson, T. (2005) *Plant Cell* **17,** 1994–2008
85. Piskounova, E., Viswanathan, S. R., Janas, M., LaPierre, R. J., Daley, G. Q., Sliz, P., and Gregory, R. I. (2008) *J. Biol. Chem.* **283,** 21310–21314
86. Narayanan, N., Gorelick, R. J., and DeStefano, J. J. (2006) *Biochemistry* **45,** 12617–12628
87. Roussell, D. L., and Bennett, K. L. (1993) *Proc. Natl. Acad. Sci. U.S.A.* **90,** 9300–9304
88. Webb, J. R., and McMaster, W. R. (1993) *J. Biol. Chem.* **268,** 13994–14002
89. Emanuelsson, O., Brunak, S., von Heijne, G., and Nielsen, H. (2007) *Nat. Protoc.* **2,** 953–971
90. Panigrahi, A. K., Ogata, Y., Zíková, A., Anupama, A., Dalley, R. A., Acestor, N., Myler, P. J., and Stuart, K. D. (2009) *Proteomics* **9,** 434–450
91. Vondrusková, E., van den Burg, J., Zíková, A., Ernst, N. L., Stuart, K., Benne, R., and Lukes, J. (2005) *J. Biol. Chem.* **280,** 2429–2438
92. Phillips, S., and Butler, J. S. (2003) *RNA* **9,** 1098–1107
93. Carneiro, T., Carvalho, C., Braga, J., Rino, J., Milligan, L., Tollervey, D., and Carmo-Fonseca, M. (2007) *Mol. Cell. Biol.* **27,** 4157–4165
94. Lange, H., Holec, S., Cognat, V., Pieuchot, L., Le Ret, M., Canaday, J., and Gagliardi, D. (2008) *Mol. Cell. Biol.* **28,** 3038–3044
95. Koslowsky, D. J., Riley, G. R., Feagin, J. E., and Stuart, K. (1992) *Mol. Cell. Biol.* **12,** 2043–2049
96. Tan, T. H., Pach, R., Crausaz, A., Ivens, A., and Schneider, A. (2002) *Mol. Cell. Biol.* **22,** 3707–3717
97. Carpousis, A. J. (2007) *Annu. Rev. Microbiol.* **61,** 71–87
98. Lykke-Andersen, S., Brodersen, D. E., and Jensen, T. H. (2009) *J. Cell Sci.* **122,** 1487–1494
99. Malecki, M., Jedrzejczak, R., Stepien, P. P., and Golik, P. (2007) *J. Mol. Biol.* **372,** 23–36
100. Taghbalout, A., and Rothfield, L. (2008) *Mol. Microbiol.* **70,** 780–782
101. Panigrahi, A. K., Zíková, A., Dalley, R. A., Acestor, N., Ogata, Y., Anupama, A., Myler, P. J., and Stuart, K. D. (2008) *Mol. Cell. Proteomics* **7,** 534–545
102. Hernandez, A., Madina, B. R., Ro, K., Wohlschlegel, J. A., Willard, B., Kinter, M. T., and Cruz-Reyes, J. (2010) *J. Biol. Chem.* **285,** 1220–1228
103. Henriksson, N., Nilsson, P., Wu, M., Song, H., and Virtanen, A. (2010) *J. Biol. Chem.* **285,** 163–170
104. Ryan, C. M., Kao, C. Y., Sleve, D. A., and Read, L. K. (2006) *Mol. Biochem. Parasitol.* **146,** 68–77
105. Riley, G. R., Corell, R. A., and Stuart, K. (1994) *J. Biol. Chem.* **269,** 6101–6108
106. Schnaufer, A., Panigrahi, A. K., Panicucci, B., Igo, R. P., Jr., Wirtz, E., Salavati, R., and Stuart, K. (2001) *Science* **291,** 2159–2162

Table S1. Oligonucleotides used in this study. Restriction sites are underlined.

Name	Sequence	Orient.
Cloning Primers		
RND RNAi f	CGGGATCCATGTTCAGGACTATAGGAATCG	sense
RND RNAi r	CCCAAGCTTTGCCTCCGTTATCACTGGTTTC	anti
RNDMHT f	CCCAAGCTTATGTTCAGGACTATAGGAATCGTG	sense
RNDMHT r	CGGGATCCATGTAAAGAATTTTCCCCCAAACG	anti
Mutagenesis Primers		
D80Afwd	CTCGCTCGATTGCTCTGGCCATCGAGGCTTTTTG	sense
D80Arev	CAAAAAGCCTCGATGGCCAGAGCAATCGAGCGAG	anti
RNase H target oligonucleotides		
9S H Target	ATTGGTGGGCAACAATACCT	anti
12S H Target	ACAAATCTGCTTTACAACGA	anti
3' rRNA oligonucleotide probes		
9S 3' Probe	ATAAATATATTAATTACTGCACGTTATT	anti
12S 3' Probe	TCAATAATCAATCCTTGCGTACTTATA	anti
qRT-PCR primers		
9S fwd	AATGCTATTAGATGGGTGTGGAA	sense
9S rev	GCTGGCATCCATTTCTGACT	anti

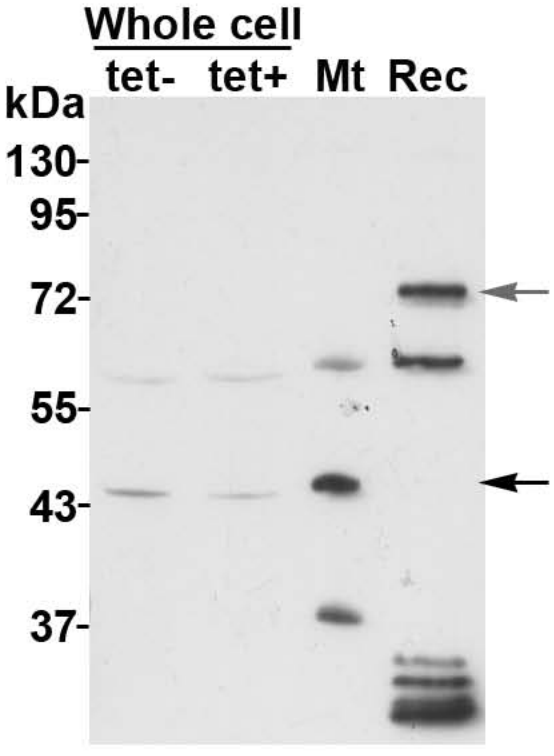

Fig. S1. **Properties of the TbRND antibody.** Entire TbRND immunoblot in which the position of native TbRND is indicated with a black arrow and the recombinant protein is indicated with a grey arrow. Loaded are whole cell protein extracts from 8 x 10^6 cells collected from uninduced (-tet) and TbRND RNAi induced (+tet) cells, protein extract from Percoll-fractionated mitochondria using 8 x 10^7 cells as starting material, and 100 ng recombinant TbRND.